JOURNAL OF AIRCRAFT
Vol. 46, No. 6, November–December 2009

Multidisciplinary Code Coupling for Analysis and Optimization of Aeroelastic Systems

Melike Nikbay,* Levent Öncü,† and Ahmet Aysan‡
Istanbul Technical University, 34469 Istanbul, Turkey

DOI: 10.2514/1.41491

This paper presents a practical methodology for static aeroelastic analysis and aeroelastic optimization via coupling of high-fidelity commercial codes. A finite-volume-based flow solver FLUENT is used to solve three-dimensional Euler equations, Gambit is used to generate mesh in the fluid domain, and CATIA is used to model parametric solid geometry. Abaqus, a structural finite element method solver, is used to compute the structural response of the aeroelastic system. The mesh-based parallel-code coupling interface MpCCI is used to exchange the pressure and displacement information between FLUENT and Abaqus to perform a loosely coupled aeroelastic analysis by a staggered algorithm, and modeFRONTIER software is used as the optimization driver for scheduling a nondominated sorting genetic algorithm initiated with design of experiments. First, an AGARD 445.6 wing configuration is optimized with objectives of maximum lift/drag ratio and minimum weight. Optimization variables are chosen as sweep angle at the quarter-chord and the taper ratio of the wing. Second, a more realistic wing model, ARW-2, is optimized for thickness values of the inner ribs and spars. Aeroelastic analysis produce consistent results with experimental data, and the applied optimization methodology results in Pareto-optimal solutions.

Nomenclature

c_{root}	=	chord of the wing root
c_{tip}	=	chord of the wing tip
$[D]$	=	damping matrix
E	=	total energy
$\tilde{F}$	=	flux vector
F_a	=	aerodynamic force
F_e	=	external force
$\tilde{F}_1, \tilde{F}_2, \tilde{F}_4$	=	Cartesian components of flux vector
$g(s)$	=	set of inequality constraints
$h(s)$	=	set of equality constraints
$[K]$	=	stiffness matrix
L/D	=	lift/drag value
M	=	total mass of the wing
$[M]$	=	mass matrix
p	=	pressure
s	=	set of optimization parameters
s_L	=	lower bound of optimization parameters
s_U	=	upper bound of optimization parameters
t_i, t_j, T_k	=	thickness parameters
u	=	structural displacement
$\dot{u}$	=	first time derivative of displacement
$\ddot{u}$	=	second time derivative of displacement
$u_{\max}$	=	maximum displacement of the wing
u_1, u_2, u_3	=	velocity components in the x, y, and z directions
W	=	weight of the wing
w	=	conservative fluid state variables
α	=	angle of attack
$\Lambda_{\frac{c}{4}}$	=	sweep angle at the quarter-chord
λ	=	taper ratio
ρ	=	fluid mass density
$\sigma_{\max}$	=	maximum von Mises stress

Presented as Paper 5876 at the 12th AIAA/ISSMO Multidisciplinary Analysis and Optimization Conference, Victoria, British Columbia, Canada, 10–12 September 2008; received 9 October 2008; revision received 19 September 2009; accepted for publication 26 September 2009.

*Assistant Professor, Astronautical Engineering Department, Faculty of Aeronautics and Astronautics, Ayazaga Campus; nikbay@itu.edu.tr. Member AIAA.

†Graduate Student, Faculty of Aeronautics and Astronautics, Ayazaga Campus. Student Member AIAA.

‡Research Assistant, Faculty of Aeronautics and Astronautics, Ayazaga Campus.

I. Introduction

AEROELASTICITY examines the multidisciplinary interaction and energy transfer between the elastic structure of an aircraft and the aerodynamic forces acting on it during flight. Catastrophic instability phenomena occur when this interaction cannot be damped. For aircraft manufacturers, the accurate prediction of aeroelastic loads is essential for structural design. Aeroelasticity requires the simultaneous analysis of fluid and structural equations and an interface to simulate the fluid–structure interaction. During the predesign phase of an aircraft, low-fidelity aeroelastic models may give reasonable load estimates in a short time, but during the detailed design phase, high-fidelity solutions and virtual prototyping capabilities are required. Computer-aided design (CAD), computational fluid dynamics (CFD), computational structural dynamics (CSD), and multidisciplinary optimization techniques can be assembled together to yield these sought-after solutions. Generally, there are three main ingredients that contribute to the improvement of the multidisciplinary optimal solution: the fidelity level of the individual analysis used inside each discipline, effectiveness of the coupling method, and computational efficiency and accuracy of the optimization algorithm.

Several works in aeroelastic optimization have been published using academic codes with high-fidelity and/or tight coupling. These include the works done by Giunta [1], Maute et al. [2–4], Nikbay [5], Moller and Lund [6], Hou and Satyanarayana [7], Gumbert et al. [8], Martins et al. [9], and Barcelos and Maute [10]. These works employed Euler/Navier–Stokes solvers for aerodynamic analysis and the finite element method for structural analysis.

Some aeroelastic analyses using commercial codes have been recently presented. Kuntz and Menter [11] used commercial software packages (high-fidelity nonlinear finite element solver ANSYS and the general-purpose finite-volume-based CFD code CFX-5) to perform an aeroelastic analysis of the AGARD 445.6 wing. A mesh-based parallel-code coupling interface (MpCCI) was used for the interfacing and data transfer between CSD and CFD solvers. Love et al. [12] used the unstructured CFD solver SPLITFLOW and the MSC.Nastran CSD solver for the aeroelastic computations of an F-16

model in a hard pull-up maneuver. They used a loosely coupled method for the analysis. Data transfers between the codes were done by using the multidisciplinary computing environment. Cavagna et al. [13] used an interfacing method that can be applied on nonmatching meshes based on moving least squares. They used FLUENT as the fluid solver and MSC.Nastran as the structural solver for the aeroelastic analysis of the AGARD 445.6 wing. They used a user-defined function to implement the grid-deformation scheme in FLUENT.

As one of the limited examples of aeroelastic optimization studies with commercial codes, Giunta and Sobieszczanski-Sobieski [14] performed aeroelastic analysis and optimization study by using government, commercial, and off-the-shelf software for the optimization of a high-speed civil transport wing. NASA Langley Research Center's finite element analysis-optimization package Genesis, Euler solver CFL3D, finite element solver MSC.Nastran, and geometry translators G/COTS were used.

However, to the best of the authors' knowledge, there has not been a published aeroelastic optimization study that uses code coupling of only commercial software packages. For industrial applications, there is still a need for modular, robust, easily accessible, affordable, and practical methodologies that can still employ high-fidelity aeroelastic analysis and advanced multidisciplinary optimization techniques. Industrial companies usually employ one software package for CAD, CFD, and CSD. Furthermore, there exists a corporate culture in which hundreds of people use the same software for many years. Thus, it is advantageous for companies to avoid the additional expense of maintaining special-purpose software modules that are infrequently used. Even for multidisciplinary optimization studies, companies are normally apt to only couple the day-to-day codes in an attach/detach manner. With this observation, in the aeroelastic optimization field, we look at the feasibility of coupling only off-the-shelf software in a modular manner. This study is an extension of the work presented by Nikbay et al. [15,16], Öncü [17], and Aysan [18].

II. Computational Framework

In this study, MpCCI [19] is used as an aeroelastic coupling interface. The advantage of using MpCCI is that it facilitates the exchange of data between nonmatching mesh interfaces of CFD and CSD codes. The staggered algorithm used in this study is given in Fig. 1. Ten aeroelastic couplings (data transfers) are performed during each optimization iteration. Abaqus version 6.7.1, a finite element analysis software, was used as the linear static structural solver. The equations of motion for a linear structure can be written as follows:

$$[M]\{\ddot{u}\} + [D]\{\dot{u}\} + [K]\{u\} = \{F_a\} + \{F_e\} \tag{1}$$

The time derivatives of Eq. (1) are neglected since the analysis is static. Also, only the aerodynamic forces are considered. Therefore, the system of linear equations can be written as

$$[K]\{u\} = \{F_a\} \tag{2}$$

Abaqus version 6.7.1 [20] calculates displacements by using the aerodynamic loads calculated from the flow solver FLUENT [21]. FLUENT version 6.3.26 can be employed for modeling fluid flow both for structured and unstructured grids by using the Navier–Stokes/Euler equations. A finite-volume-based approach is used to define the discrete equations. The fluid solver solves the governing equations of continuity, momentum, and energy simultaneously. In this study, the flow was assumed to be inviscid and the Euler equations in Eq. (3) were used. This is a valid approximation for high Reynolds number flows according to Prandtl's boundary-layer analysis. Moreover, according to Barcelos and Maute [10], inviscid flow models give acceptable results for maximizing the lift/drag optimization problems in transonic cruise conditions. In conservative form, the 3-D Euler equations are written as

$$\frac{\partial w}{\partial t} + \nabla.\tilde{F}(w) = 0 \tag{3}$$

The conservative fluid state variable w is defined as

$$w = \begin{pmatrix} \rho \\ \rho u_1 \\ \rho u_2 \\ \rho u_3 \\ E \end{pmatrix} \tag{4}$$

where ρ is the fluid density; u_1, u_2, and u_3 are three velocities; and E is the total internal energy per mass. The flux $\tilde{F}$, has three components ($\tilde{F}_1$, $\tilde{F}_2$, and $\tilde{F}_3$), as follows:

$$\tilde{F}_1 = \begin{pmatrix} \rho u_1 \\ \rho u_1^2 + p \\ \rho u_1 u_2 \\ \rho u_1 u_3 \\ (E+p)u_1 \end{pmatrix} \quad \tilde{F}_2 = \begin{pmatrix} \rho u_2 \\ \rho u_2 u_1 \\ \rho u_2^2 + p \\ \rho u_2 u_3 \\ (E+p)u_2 \end{pmatrix}$$

$$\tilde{F}_3 = \begin{pmatrix} \rho u_3 \\ \rho u_3 u_1 \\ \rho u_3 u_2 \\ \rho u_3^2 + p \\ (E+p)u_3 \end{pmatrix} \tag{5}$$

where p is the fluid pressure.

III. Aeroelastic Analysis of AGARD 445.6 Wing

The weakened model of the AGARD 445.6 wing [22] is considered here. The finite element model in Abaqus is composed of 19,610 linear hexahedral structural elements.

The computational grid of the flow domain was constructed in Gambit with 691,000 tetrahedral elements and 1.35 million faces. The flow is modeled with the Euler equations. The freestream Mach number was set to 0.85 and the angle of attack was 5 deg.

For aeroelastic analysis, MpCCI was used to transfer the aeroelastic data (surface pressures from the CFD and nodal displacements from the CSD) between the CFD and CSD models of the wing. The aeroelastic results were compared to the results of Cai et al. [23]. The pressure contours on the upper surface of the wing are shown in Fig. 2. The reference result is shown on the left and the current result is shown on the right side of Fig. 2. As seen from the figures, the pressure contours are comparable with the reference results. Moreover, the pressure coefficient distributions at 67% span are shown in Fig. 3. The x axis of the figures show the points along the chord from the leading edge. The current results on the right agree

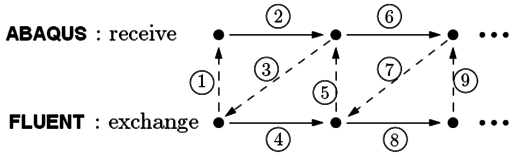

Fig. 1 Staggered algorithm for the aeroelastic coupling [19].

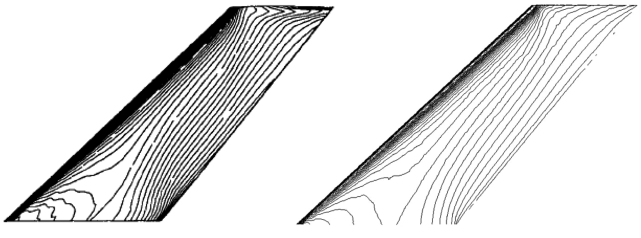

Fig. 2 Pressure distributions on the upper wing surface.

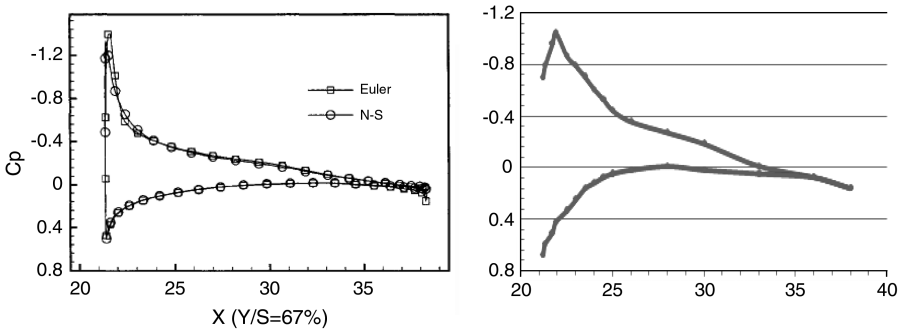

Fig. 3 Pressure coefficient distribution at 67% span (*X* in inches).

well with the reference results, except for the leading-edge suction sections for the upper wing surface. This difference can be the result of the mesh type or different solvers used in these two studies. The last compared result is vertical deflection of the wing along the span relative to the wing root. The comparison of deflection results is shown in Fig. 4. As seen from Fig. 4, the out-of-plane deformation behavior for the wing agrees well with the results of Cai et al. [23]. There are slight differences for the leading-edge section. This can be due to the different methods used in the two different studies. In the present study, a 3-D finite element analysis software is used to find the displacement values, whereas Cai et al. [23] used a modal structural method in order to predict the displacement values.

IV. Aeroelastic Optimization of AGARD 445.6 Wing

In this study, multi-objective and multidisciplinary optimization of the AGARD 445.6 wing configuration will be performed by using modeFRONTIER software [17].

A. Formulation of Optimization Problem

Taper ratio and the quarter-chord sweep angle are selected as the design variables for the AGARD 445.6 wing. When these variables are changed, the fiber orientation on the structural model, the average chord, and the planform-area values also change. The latter three variables are not used as direct optimization variables; instead, they are recalculated according to the values of sweep angle and taper ratio. In this problem, the only given constraint is the maximum deformation of the wing tip due to the aerodynamic loads over the wing. The deformation at the tip is constrained to one-tenth of the wing span. Finally, there are two objective functions in this problem, which are maximizing the lift/drag ratio and minimizing the weight. The drag considered here is the induced drag. For multi-objective optimization problems, the optimization driver will try to find the Pareto-optimal set. The overall optimization problem with two objectives can be formulated as

$$\min_{s\epsilon S} M(\boldsymbol{s}) \quad \text{and} \quad \max_{s\epsilon S} \frac{L}{D}(\boldsymbol{s}) \tag{6}$$

$$g(\boldsymbol{s}) = \frac{u_{\max}}{76\ \text{mm}} - 1.0 \le 0 \qquad g(\boldsymbol{s}) \in \mathbb{R}^1 \tag{7}$$

$$\boldsymbol{S} = \{\boldsymbol{s} \in \mathbb{R}^2 | \boldsymbol{s}_L \le \boldsymbol{s} \le \boldsymbol{s}_U\} \qquad \boldsymbol{s} = (\lambda, \Lambda_{\frac{c}{4}})$$
$$0.1 \le \lambda \le 0.5 \qquad 0\,\text{deg} \le \Lambda_{\frac{c}{4}} \le 50\,\text{deg} \tag{8}$$

where $M(\boldsymbol{s})$ is the total mass of the wing, $(L/D)(\boldsymbol{s})$ is the lift/drag value for the wing, $u_{\max}$ is the maximum deformation of the wing tip, λ is the taper ratio defined as $\lambda = c_{\text{tip}}/c_{\text{root}}$, and $\Lambda_{\frac{c}{4}}$ is the sweep value at the quarter-chord. The modeFRONTIER software has both gradient-based and gradient-free algorithms. In this work, the multi-objective genetic algorithm MOGA [24] was chosen as the driver. The scheduler used in this study is the nondominated sorting genetic algorithm (NSGA-II) [25] that was implemented by Deb et al. [26]. This is a fast and advanced multi-objective evolutionary algorithm. A multi-objective optimization algorithm tries to find the components of a vector-valued objective function. Thus, the solution is a set of solutions called a Pareto-optimal set. Every Pareto-optimal point in the set is an equally acceptable solution for a multi-objective optimization problem [25].

B. Optimization Framework

Several commercial software codes were coupled during the optimization process in this problem. FLUENT version 6.3.26 is used to solve inviscid 3-D Euler equations, Gambit is used to generate the fluid-domain mesh generator, and CATIA-V5-R16 is used to model the parametric 3-D solid. Abaqus version 6.7.1 was used to compute the structural response of the aeroelastic system. Mesh-based parallel-code coupling interface MpCCI-3.0.6 was used to exchange the pressure and displacement information between FLUENT and Abaqus. The modeFRONTIER software version 4.0 was used as a multi-objective and multidisciplinary optimization software to automate the workflow shown in Fig. 5.

In Fig. 5, the optimization variables (their limits and increments), optimization algorithm (scheduler), design of experiments, objectives, constraints, output variables, and software are defined. At every optimization iteration, the workflow is run from the beginning with the changes in design. Once the workflow is run, it controls the optimization process automatically by using prepared script files and models. This feature provides an automatic communication to update all the input files (geometry and analysis) and run all the codes in batch mode.

The optimization process in Fig. 5 flows from left to right. The scheduler NSGA-II updates the design variables and at the beginning of each optimization iteration. The CSD and CFD branches of the

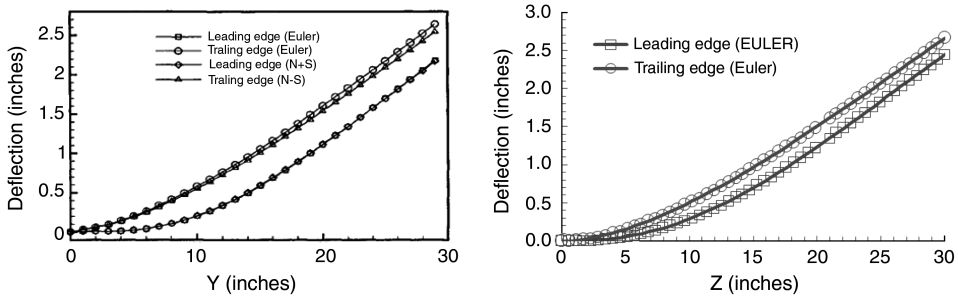

Fig. 4 Vertical deflection of the wing along the span relative to the wing root.

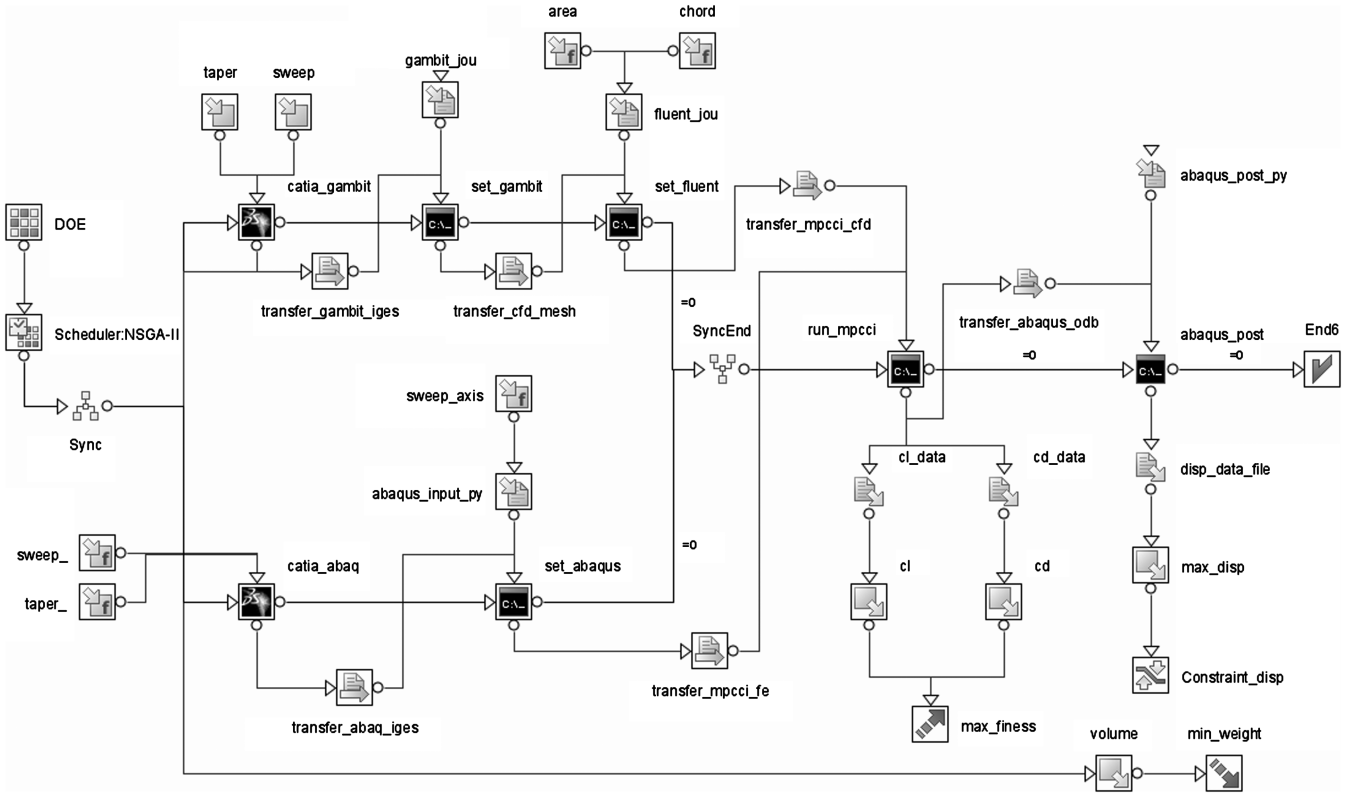

Fig. 5 Aeroelastic optimization workflow for AGARD 445.6 wing.

workflow prepare input files separately, so they need to be synchronized for aeroelastic analysis. In the upper branch, which is the CFD part, the CATIA version 5 node changes optimization variables by using the parametric CAD model. The geometric model is transferred to Gambit in initial graphics exchange specification (iges) format. Gambit uses a journal file to prepare the fluid mesh and to update the boundary conditions and then transfers the mesh file to FLUENT. FLUENT updates the optimization variables and imports the mesh files. FLUENT prepares the flow model and sets boundary conditions through a journal file and transfers the case file to MpCCI for the aeroelastic analysis. The lower branch in Fig. 5 shows CSD preprocessing. Again, the CATIA version 5 node updates the optimization variables by using the parametric CAD model. Abaqus updates the structural model by using a Phyton script and transfers the input file to MpCCI for the aeroelastic analysis. Then MpCCI performs the coupling by using the FLUENT and Abaqus models in batch mode. This aeroelastic analysis produces a result file that contains the aerodynamic and structural criteria. The modeFRONTIER software controls the constraint violation. NSGA-II controls the optimization process and, if needed, a new iteration process starts.

C. Optimization Results

In this problem, 12 designs of experiment (DOE) (with a Sobol sequence that is capable of distributing the experiments uniformly in the design space [25]) and 17 generations for the NSGA-II were defined. A total of 204 designs were generated for the optimization problem. The solution of the problem took 23 h and 51 min on a workstation configured with Microsoft Windows XP operating system, a Core2Duo with 2.66 GHz, and 2 GB of RAM.

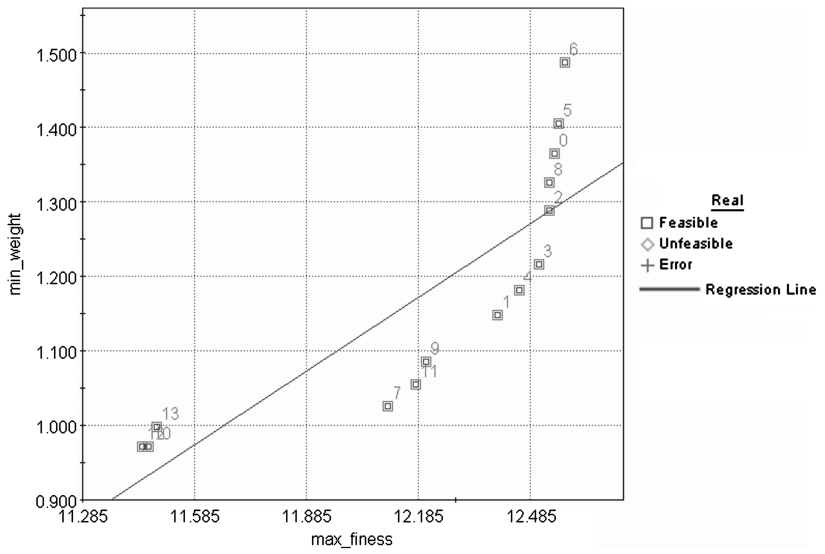

Fig. 6 Scatter-chart minimum weight vs maximum L/D.

Table 1 Pareto designs

Pareto	Sweep	Taper	C_d	C_l	Max fitness	Min weight, kg	Displacement, mm
6	38	0.475	0.0295	0.3706	12.5754	1.4885	60.6254
9	32	0.200	0.0350	0.4274	12.2043	1.0853	70.6557
10	6	0.100	0.0405	0.4640	11.4589	0.9715	57.9876

The optimization analysis showed that 78 designs (72% of all designs) were found to be feasible (i.e., satisfy the constraint condition given in the optimization problem), and 26 designs (24% of all designs) were unfeasible. Moreover, there were four error designs (4% of all designs) that did not give any solution because of modeling or computational errors in the optimization workflow.

Furthermore, 14 designs were found in the Pareto-front set for this optimization problem. All of these designs are feasible optimum solutions but with different weights for the corresponding objectives. For example, an aerodynamics engineer may prefer the design with maximum lift/drag ratio, whereas a structural engineer can choose the design with minimum weight. The relations between the objectives are given in the scatter chart in Fig. 6. As seen from Fig. 6, the relationship between the objectives of maximum lift/drag ratio and minimum weight is nonlinear. A quadratic function can describe this relationship.

As a result of this study, three designs can be recommended from the Pareto-optimal set of 14 designs, as shown in Table 1. Design number 6 is the best solution for maximum L/D value, design number 10 is the best solution for minimum weight, and design number 9 is an intermediate design.

V. Aeroelastic Optimization of ARW-2 Wing

After the code coupling approach is tested for a simple geometry, an aeroleastic optimization study based on a more realistic wing model called the aeroelastic research wing (ARW-2) [27,28] is performed. NASA's experimental ARW-2 wing skin is made of a fiberglass material with honeycomb panels sandwiched between the middle two layers of fiberglass. In this study, the wing skin is modeled with an isotropic skin instead of composite skin, for the sake of simplicity. The corresponding material and geometrical properties are identified so that both structural and aeroelastic responses are consistent with the experimental data in a former work by Nikbay and Aysan [16]. The computational ARW-2 wing model consists of 17 ribs, 5 spars, and 4 axial bars, as shown in Fig. 7.

A. Formulation of Aeroelastic Optimization Problem

A generic optimization problem from the literature is chosen [3]. The objectives are maximizing lift/drag ratio and minimizing the weight of the wing. The optimization variables are the thicknesses of all ribs and spars and the angle of attack. There were three aeroelastic constraints. The first constraint imposes that the maximum deformation of the wing tip is 0.381 m. The second constraint requires that the lift L can vary only by an amount greater or equal to the variation of the weight induced by the variation of the thicknesses of the structural elements. The third constraint limits the von Mises stress to a maximum of 9.05×10^7 Pa. The optimization problem is formulated as

$$\min_{s\epsilon S} W(\boldsymbol{s}), \qquad \max_{s\epsilon S} \frac{L}{D}(\boldsymbol{s}) \tag{9}$$

$$g_1(\boldsymbol{s}) = \frac{2\Delta W(\boldsymbol{s})}{\Delta L(\boldsymbol{s})} - 1 \le 0 \qquad g_1(\boldsymbol{s}) \in \mathbb{R} \tag{10}$$

$$g_2(\boldsymbol{s}) = \frac{u_{\max}(\boldsymbol{s})}{0.381\ \text{m}} - 1 < 0 \qquad g_2(\boldsymbol{s}) \in \mathbb{R} \tag{11}$$

$$g_3(\boldsymbol{s}) = \frac{\sigma_{\max}(\boldsymbol{s})}{9.05 \times 10^7\ \text{Pa}} - 1 \le 0 \qquad g_3(\boldsymbol{s}) \in \mathbb{R} \tag{12}$$

$$\boldsymbol{s} = (\alpha, k_1, k_2, k_3) \qquad -2 \le \alpha \le 6$$
$$-0.25 \le k_1, k_2, k_3 \le 0.25 \tag{13}$$

where $W(\boldsymbol{s})$ is the total weight of the wing; $(L/D)(\boldsymbol{s})$ is the lift/drag value for the wing; $u_{\max}$ is the maximum deflection at the wing tip; $\Delta L(\boldsymbol{s})$ is the change in the lift of the wing; $\Delta W(\boldsymbol{s})$ is the change in the weight of the wing; $\sigma_{\max}(\boldsymbol{s})$ is the maximum von Mises stress; α is the angle of attack; and k_1, k_2, and k_3 are the abstract optimization parameters used to vary the thicknesses of the ribs t_i and t_j and spars T_k. To decrease the number of optimization variables, 17 ribs were grouped into two groups as follows. The first half has an index i, and the second half has an index j. At the $(n+1)$th optimization iteration, the values of all the thickness variables were updated by three optimization variables as follows:

$$t_i^{(n+1)} = t_i^{(0)} + t_i^{(0)} \cdot k_1^{(n+1)} \qquad i = 1, 2, \ldots, 7 \tag{14}$$

$$t_j^{(n+1)} = t_j^{(0)} + t_j^{(0)} \cdot k_2^{(n+1)} \qquad j = 8, 9, \ldots, 17 \tag{15}$$

$$T_k^{(n+1)} = T_k^{(0)} + T_k^{(0)} \cdot k_3^{(n+1)} \qquad k = 1, 2, \ldots, 5 \tag{16}$$

where $t_i^{(0)}$, $t_j^{(0)}$, and $T_k^{(0)}$ are the thickness values for the ribs and spars at the initial design.

Figure 8 shows the workflow of this optimization problem. The methodology is the same as the previous problem. Multi-objective genetic algorithm MOGA was chosen as the optimization driver. The scheduler used is the nondominated sorting genetic algorithm NSGA-II [25]; modeFRONTIER's script files were used to drive Abaqus and FLUENT codes in batch mode. For each optimization iteration, modeFRONTIER updates the thickness parameters of the wing and creates a new input file for Abaqus, updates the angle of attack parameter, and creates a new mesh and case file for FLUENT. The weight criterion is a direct output of the Abaqus node. During the fluid–structure interaction iterations, MpCCI exchanges the displacement and pressure values between Abaqus and FLUENT before Abaqus finally evaluates the displacement criteria.

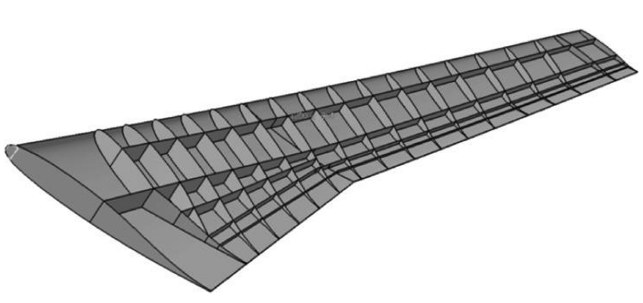

Fig. 7 Computational model of ARW-2 wing structure.

B. Optimization Results

In this study, six DOE with a Sobol sequence are used and 34 generations for the MOGA-II are defined. Finally, a total of 129 designs are generated for the optimization problem. The solution of

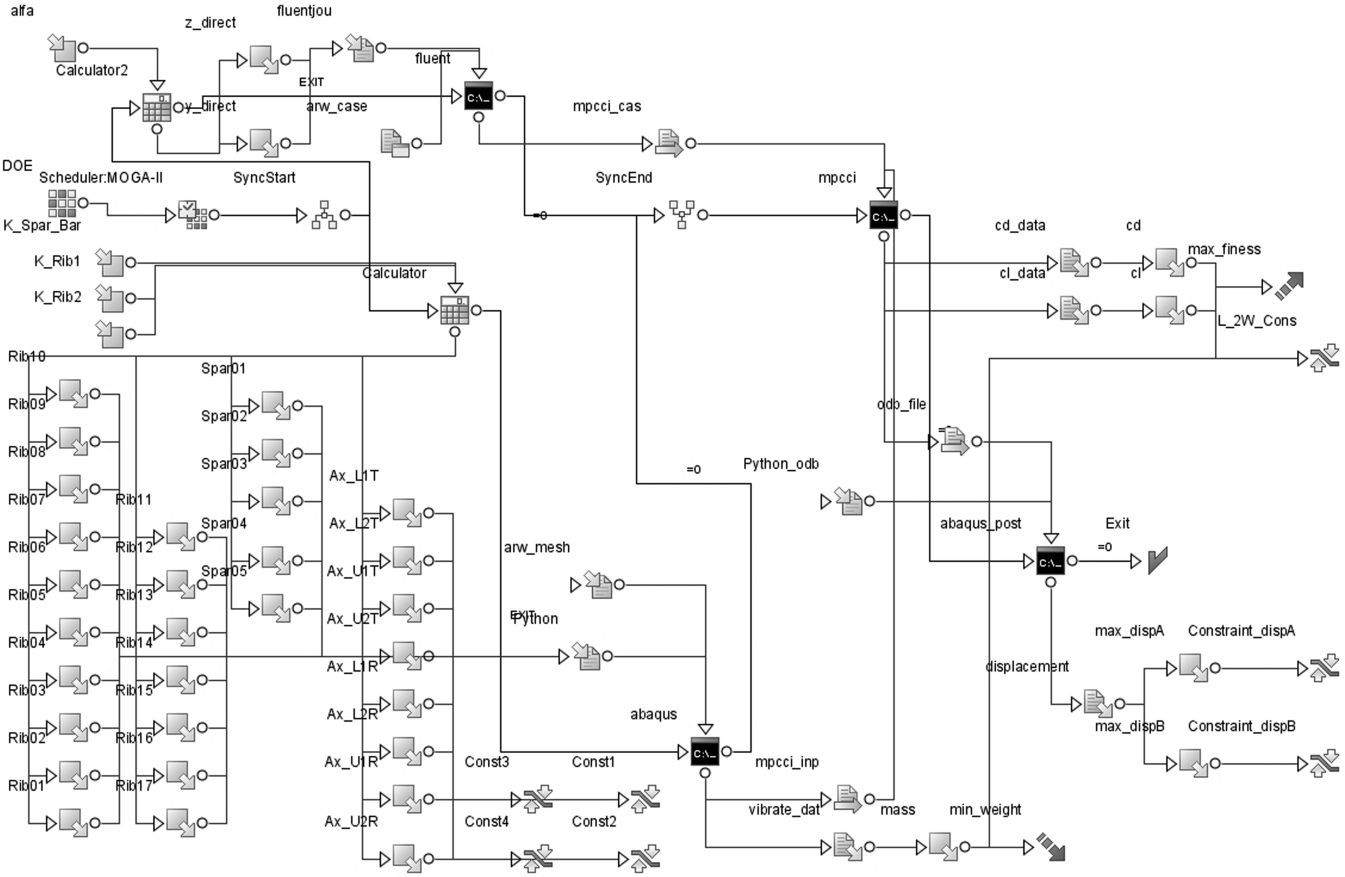

Fig. 8 Aeroelastic optimization workflow for ARW-2 wing.

the problem took 188 h on a workstation configured with an Intel Core2 CPU 6700 with a 2.66 GHz processor, 2 GB of RAM, and the Microsoft Windows XP operating system. The results showed that 36 designs were found to be feasible (i.e., satisfy the constraint condition given in the optimization problem) and 12 designs were unfeasible (i.e., did not satisfy the constraint condition). Moreover, there were nine error designs that did not give any solution because of modeling or computational errors resulting from the optimization workflow. Finally, two designs were found in the Pareto-optimal set for this optimization problem. These Pareto designs are shown in Table 2. One of the Pareto designs is preferred as the best wing configuration due to its lower weight value. Table 3 shows a comparison between the initial and optimum design of ARW-2 wing by weighting the two objectives equally.

Table 2 Pareto-optimal designs

Angle of attack α	k_1	k_2	k_3	L/D	Weight N
0	−0.22	−0.25	−0.25	11.836	507.42
0	−0.08	0.23	−0.25	11.836	561.81

Table 3 Performance improvements by optimization

	Angle of attack α	k_1	k_2	k_3	L/D	Weight N
Initial design	2.5	0	0	0	10.76	597.284
Optimum design	0	−0.22	−0.25	−0.25	11.836	507.42
Improvements	——	——	——	——	9.09%	15.04%

VI. Conclusions

The previous works published in aeroelastic analysis and optimization field mostly rely on academic or in-house-developed codes. For industrial applications, there is a need for modular, robust, easily accessible, affordable, and practical methodologies that can be incorporated for estimation of aeroelastic loads in detailed-design phases. This work presented a computer-aided design, computational fluid dynamics, and computational-structural-dynamics-based high-fidelity multidisciplinary optimization methodology by using a code-coupling approach that uses only off-the-shelf commercial codes. Frequently used codes such as CATIA, Abaqus, Gambit, and FLUENT are coupled with more advanced drivers such as MpCCI and modeFRONTIER. The multidisciplinary design process is completely automatized by the implementation of an optimization workflow that calls the analysis codes in batch mode. At each optimization iteration, the changes in design are transferred automatically to input files (including geometry, fluid mesh, structural mesh, and analysis inputs) by scripts. The methodology was tested for static aeroelastic analysis and optimization using the AGARD 445.6 and ARW-2 wings. The results in both cases were found to be feasible.

This approach can be used in an attach/detach mode with any other commercial software that are needed to replace one of the codes used in this framework. Since this methodology uses an advanced computer-aided design tool, it will be compatible for virtual prototyping applications to reduce the time and cost of the product development phase. The approach can be employed in any industrial application with no restrictions. This optimization process can be connected to any other computer-aided engineering process with some effort.

The study can be applied to more detailed aircraft structures and problems with more design variables with the parallelization of the optimization workflow. Aeroelastic tailoring with addition of composite models into the framework and optimization based on

dynamic aeroelastic analysis are some examples of the appealing work that can be accomplished by using the developed methodology.

Acknowledgments

The three authors of this paper would like to thank TUBITAK (The Scientific and Technological Research Council of Turkey) for the research fund provided through 3501 National Young Researchers Career Development Program for the project titled "Analysis and Reliability Based Design Optimization of fluid–structure Interaction Problems Subject to Instability Phenomena" with grant number 105M235. The three authors would like to thank Istanbul Technical University Informatics Institute High Performance Computing Laboratory. The first author would like to thank to Thuan Lieu for reviewing this paper.

References

[1] Giunta, A., "A Novel Sensitivity Analysis Method for High-Fidelity Multidisciplinary Optimization of Aero-Structural Systems," AIAA, 38th Aerospace Science Meeting and Exhibit, Paper 2000-0683, Reno, NV, Jan. 2000.

[2] Maute, K., Nikbay, M., and Farhat, C., "Coupled Analytical Sensitivity Analysis for Aeroelastic Optimization," AIAA, 8th AIAA/USAF/NASA/ISSMO Symposium on Multidisciplinary Analysis and Optimization, Paper 2000-4825, Long Beach, CA, Sept. 2000.

[3] Maute, K., Nikbay, M., and Farhat, C., "Coupled Analytical Sensitivity Analysis and Optimization of Three-Dimensional Nonlinear Aeroelastic Systems," *AIAA Journal*, Vol. 39, No. 11, 2001, pp. 2051–2061. doi:10.2514/2.1227

[4] Maute, K., Nikbay, M., and Farhat, C., "Sensitivity Analysis and Design Optimization of Three-Dimensional Nonlinear Aeroelastic Systems by the Adjoint Method," *International Journal for Numerical Methods in Engineering*, Vol. 56, No. 6, Feb. 2003, pp. 911–933. doi:10.1002/nme.599

[5] Nikbay, M., "Coupled Sensitivity Analysis by Discrete-Analytical Direct and Adjoint Methods with Applications to Aeroelastic Optimization and Sonic Boom Minimization," Ph.D. Thesis, Univ. of Colorado at Boulder, Boulder, CO, 2002.

[6] Moller, H., and Lund, E., "Shape Sensitivity Analysis of Strongly Coupled Fluid–Structure Interaction Problems," AIAA, 8th AIAA/USAF/NASA/ISSMO Symposium on Multidisciplinary Analysis and Optimization, Paper 2000-4825, Long Beach, CA, Sept. 2000.

[7] Hou, G.-W., and Satyanarayana, A., "Analytical Sensitivity Analysis of a Statical Aeroelastic Wing," AIAA, 8th AIAA/USAF/NASA/ISSMO Symposium on Multidisciplinary Analysis and Optimization, Paper 2000-4825, Long Beach, CA, Sept. 2000.

[8] Gumbert, C., Hou, G.-W., and Newman, P., "Simultaneous Aerodynamic Analysis and Design Optimization (SAADO) for a 3-D Flexible Wing," AIAA, 43rd AIAA/ASME/ASCE/AHS/ASC Structures, Structural Dynamics, and Materials Conference, Paper 2002-1483, Denver, CO, April 2002.

[9] Martins, J., Alonso, J., and Reuther, J., "High-Fidelity Aero-Structural Design Optimization of a Supersonic Business Jet," AIAA, 43rd AIAA/ASME/ASCE/AHS/ASC Structures, Structural Dynamics, and Materials Conference, Paper 2002-1483, Denver, CO, April 2002.

[10] Barcelos, M., and Maute, K., "Aeroelastic Design Optimization for Laminar and Turbulent Flows," *Computer Methods in Applied Mechanics and Engineering*, Vol. 197, Nos. 19–20, 2008, pp. 1813–1832. doi:10.1016/j.cma.2007.03.009

[11] Kuntz, M., and Menter, F., "Simulation of Fluid–Structure Interactions in Aeronautical Applications," *European Congress on Computational Methods in Applied Sciences and Engineering ECCOMAS 2004*, edited by P. Neittaanmäki, T. Rossi, S. Korotov, E. Oñate, J. Périaux, and D. Knörzer, 24–28 July 2004, pp. 133–144.

[12] Love, M., De La Garza, T., Charlton, E., and Egle, D., "Computational Aeroelasticity in High Performance Aircraft Flight Loads," *22nd International Congress of Aeronautical Sciences (ICAS 2000)*, 2000.

[13] Cavagna, L., Quaranta, G., Mantegazza, P., Merlo, E., Marchetti, D., and Martegani, M., "Preliminary Assessment of the Complete Aeroelastic Simulation of the M-346 in Transonic Condition with a CFD Navier–Stokes Solver," *L'Aerotecnica, Missili e Spazio*, Vol. 84, No. 3, 2005, pp. 115–127.

[14] Giunta, A., and Sobieszczanski-Sobieski, J., "Progress Towards Using Sensitivity Derivatives in a High-Fidelity Aeroelastic Analysis of a Supersonic Transport," AIAA, 7th AIAA/USAF/NASA/ISSMO Symposium on Multidisciplinary Analysis and Optimization, Paper 98-4763, St. Louis, MO, Sept. 1998, pp. 441–453.

[15] Nikbay, M., Öncü, L., and Aysan, A., "A Multi-Disciplinary Code Coupling Approach for Analysis and Optimization of Aeroelastic Systems," AIAA, 12th AIAA/ISSMO Multidisciplinary Analysis and Optimization Conference, Paper 2008-5876, Victoria, British Columbia, Canada, 12–13 Sept. 2008.

[16] Nikbay, M., and Aysan, A., "Identification of Structural and Aeroelastic Properties of a Computational ARW-2 Wing Model for Aeroelastic Optimization Applications," 2009 International Forum on Aeroelasticity and Structural Dynamics, Paper IFASD-2009-079, Seattle, WA, 21–25 June 2009.

[17] Öncü, L., "Multidisciplinary Design Optimization of Aerospace Structures with Static Aeroelastic Criteria," M.S. Thesis, Istanbul Technical Univ., Istanbul, Turkey, 2008.

[18] Aysan, A., "Structural Identification and Static Aeroelastic Optimization of ARW-2 Wing with Multidisciplinary Code Coupling," M.S. Thesis, Istanbul Technical Univ., Istanbul, Turkey, 2009.

[19] MpCCI, Software Package, Ver. 3.0.6, Fraunhofer Institute for Algorithms and Scientific Computing, Sankt Augustin, Germany, 2007.

[20] Abaqus, Software Package, Ver. 6.7.1, Simulia, 2007.

[21] FLUENT, Software Package, Ver. 6.3.26 ANSYS, Inc., Canonsburg, PA, 2006.

[22] Yates, E., "AGARD Standard Aeroelastic Configurations for Dynamic Response I-Wing 445.6," AGARD Rept. 765, Neuilly-sur-Seine, France, 1985.

[23] Cai, J., Liu, F., and Tsai, H., "Static Aero-Elastic Computation with a Coupled CFD and CSD Method," AIAA, 39th AIAA Aerospace Sciences Meeting and Exhibit, Paper 2001-717, Reno, NV, 8–11 Jan. 2001.

[24] Sasaki, D., Obayashi, S., and Nakahashi, K., "Navier–Stokes Optimization of Supersonic Wings with Four Objectives Using Evolutionary Algorithm," *Journal of Aircraft*, Vol. 39, No. 4, 2002, pp. 621–629. doi:10.2514/2.2974

[25] modeFRONTIER, Software Package, Ver. 4, ESTECO, Miami, FL, 2008.

[26] Deb, K., Pratap, A., Agarwal, S., and Meyarivan, T., "A Fast and Elitist Multi-Objective Genetic Algorithm NSGA-II," Kanpu Genetic Algorithms Lab., Rept. 2000001, 2000.

[27] Sandford, M., Seidel, D., Escktrom, C., and Spain, C., "Geometrical and Structural Properties of an Aeroelastic Research Wing (ARW-2)," NASA TM 4110, 1989.

[28] Sandford, M., Seidel, D., and Escktrom, C., "Steady Pressure Measurements on an Aeroelastic Research Wing (ARW-2)," NASA TM 109046, 1994.